ChemComm

COMMUNICATION

View Article Online
View Journal | View Issue

Cite this: *Chem. Commun.*, 2020, **56**, 14404

Received 8th October 2020,
Accepted 28th October 2020

DOI: 10.1039/d0cc06716d

rsc.li/chemcomm

Characterization of heterogeneous aryl–Pd(II)–oxo clusters as active species for C–H arylation†

Taeil Shin,‡[a] Minjun Kim,‡[a] Younjae Jung,[a] Sung June Cho,*[b] Hyunwoo Kim*[a] and Hyunjoon Song*[a]

C–H arylation with heterogeneous palladium was investigated. The surface oxidation of Pd nanoparticles with a hypervalent iodine reagent, $[Ph_2I]BF_4$, resulted in the generation of Pd(II)–aryl–oxo clusters, which were characterized as the crucial intermediate.

There is a long-standing debate for actual catalytic mechanisms through homogeneous and heterogeneous pathways in various organic transformations, while even using homogeneous precursors.[1–3] The formation of small Pd nanoparticles (NPs) has been reported during the Pd-catalyzed cross-coupling reactions including Suzuki–Miyaura, Sonogashira, and Mizoroki–Heck reactions.[4–10] The Pd NPs could be yielded by the aggregation of homogeneous Pd precursors, such as $Pd(OAc)_2$ (OAc = acetate) and $Pd(dba)_2$ (dba = dibenzylideneacetone). Recently, *in situ* formation of Pd NPs has been identified after the catalytic C–H bond functionalization.[11–14] It has been proposed that the heterogeneous surface potentially catalyzed the reactions on the basis of multiple control experiments. For instance, Glorius and co-workers reported the regioselective arylation of thiophenes and polyaromatic hydrocarbons using Pd/C in the presence of hypervalent iodine(III) reagents.[15,16] The reaction mechanism was proposed to use heterogeneous Pd(0) and Pd(II) species similar to the homogeneous counterpart.[15–17] However, "Pd(II) NPs" is not a proper term for the intermediates considering the strong electrostatic repulsion between Pd(II) species. It is still rarely explored what the actual catalytic species are in the heterogeneous reactions.

The metal NPs have been commonly used for low-valent transition metal catalysis due to their zero-valent nature. Recently, Toste and Somorjai expanded the heterogeneous catalysis into high-valent metal chemistry that the homogeneous counterparts usually carried out.[18–21] We have also characterized high valent nanostructures such as Pd(II), Pd(IV), and Rh(III), and investigated various organic transformations, hydroalkoxylation, coupling of epoxides and CO_2, and C–H halogenation. Moreover, Pd nanocatalysts were used for a tandem C–H halogenation and cross-coupling reaction, mediated by heterogeneous Pd(0) and Pd(IV) catalysts.[22,23]

In the present study, we revisited the Pd NPs-catalyzed C–H arylation reaction of indoles and other heterocycles, and characterized the "heterogeneous" surface intermediates. By various spectroscopic analyses, the active species were characterized to be aryl–Pd(II)–oxo clusters bearing Pd(II)–C bonds on their surface, which were used to demonstrate the plausible heterogeneous Pd(0)/Pd(II) reaction mechanisms.

To identify the heterogeneous species in the Pd NPs-catalyzed C–H arylation, we have synthesized uniform Pd NPs by thermal decomposition of Pd–oleylamine complex according to the literature.[24] The transmission electron microscopy (TEM) image shows that the particles are uniformly spherical and highly monodisperse with an average diameter of 4.2 ± 0.4 nm (Fig. 1a). The X-ray diffraction (XRD) shows a single broad peak at 40°, corresponding to the (111) reflection of Pd face-centered-cubic structure (JCPDS No. 46-1043) (Fig. S1, ESI†). The average domain size was estimated to be 4.7 nm from the FWHM of the (111) peak by using the Debye–Scherrer equation.[25]

Before the reaction study, proper solvents were selected using the Pd NPs treated with diphenyliodonium salt. In ethanol, the Pd NPs were leached out and agglomerated due to high solvent polarity (Fig. S2, ESI†). In contrast, the Pd NPs were stable in THF, maintaining its original colloidal morphology (Fig. 1b).

The reaction conditions of the C–H arylation of indole were screened in the presence of the Pd NPs and $[Ph_2I]BF_4$ (Table 1). Under the standard condition, the arylation selectively occurred at the C2-position of indole (**1b**) with 91% and 81% yields in ethanol and THF, respectively (Table 1, entries 1 and 2).

Interestingly, homogeneous Pd(II) reagents, $PdCl_2$, $Pd(TFA)_2$, and $Pd(OAc)_2$ showed superior reactivity to the Pd NPs (Table S1, ESI†), but provided the products with moderate yields (42–72%).

[a] *Department of Chemistry, Korea Advanced Institute of Science and Technology (KAIST), Daejeon 34141, Republic of Korea. E-mail: hwkim@kaist.edu, hsong@kaist.ac.kr*

[b] *Department of Chemical Engineering, Chonnam National University, Gwangju 61186, Republic of Korea. E-mail: sjcho@chonnam.ac.kr*

† Electronic supplementary information (ESI) available. See DOI: 10.1039/d0cc06716d

‡ These authors contributed equally to this work.

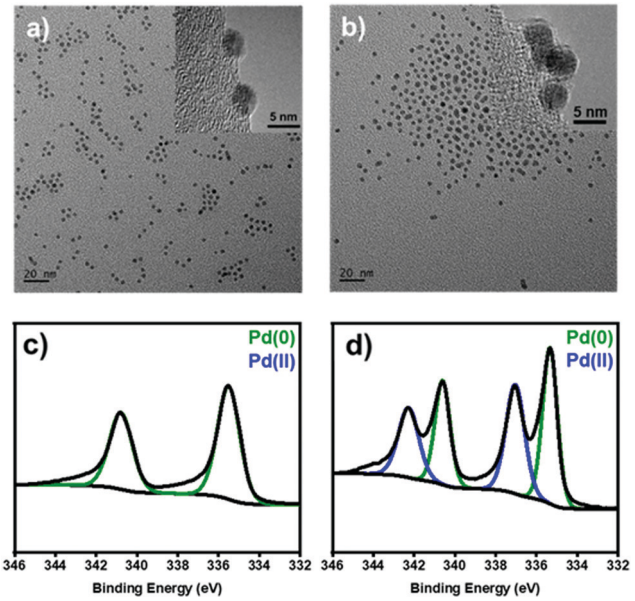

Fig. 1 (a and b) TEM images and (c and d) XPS spectra at the Pd 3d level of (a and c) the pristine and (b and d) oxidized Pd NPs after the treatment with $[Ph_2I]BF_4$.

Table 1 Arylation of indole with diaryliodonium salt catalyzed by homo- and heterogeneous Pd sources

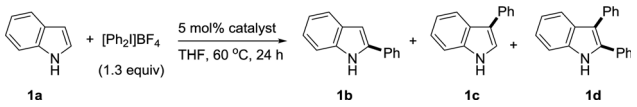

No.[a]	Catalyst	Solvent	Yield (%)	Selectivity[b] (%) 1b	1c	1d
1	Pd NPs	EtOH	91	99	—	—
2	Pd NPs	THF	80	99	—	—
3	$PdCl_2$	THF	42	80	10	10
4	$Pd(TFA)_2$	THF	47	81	18	1
5	$Pd(OAc)_2$	THF	65	76	12	12
6	$Pd(OAc)_2$	EtOH	72	76	7	17

[a] Conditions: indole (0.2 mmol) $[Ph_2I]BF_4$ (0.26 mmol) and solvent (2.0 mL) without exclusion of air and moisture. [b] Determined by gas chromatography-mass spectrometry (GC-MS) analysis. Mesitylene was used as an internal standard.

However, significant amounts of the arylation also occurred at the C3 position (**1c**) and biarylation at the C2 and C3 positions (**1d**) (Table 1, entries 3–6). The homogeneous Pd catalysts showed a large difference in reactivity and selectivity compared to the heterogeneous Pd NPs. However, the two reaction pathways are not clearly distinguished because the heterogeneous Pd was formed after the reaction with $Pd(TFA)_2$ or $Pd(OAc)_2$ (Fig. S3, ESI†).[26]

We next investigated the reaction scope of the Pd NPs-catalyzed C–H arylation of heterocyclic compounds (Scheme 1). The heterocyclic substrate was heated at 60 °C for 24 h with 1.3 equiv. of $[Ph_2I]BF_4$ and 5 mol% of Pd NPs in THF. Under the reaction condition, N-heterocyclic compounds including indole

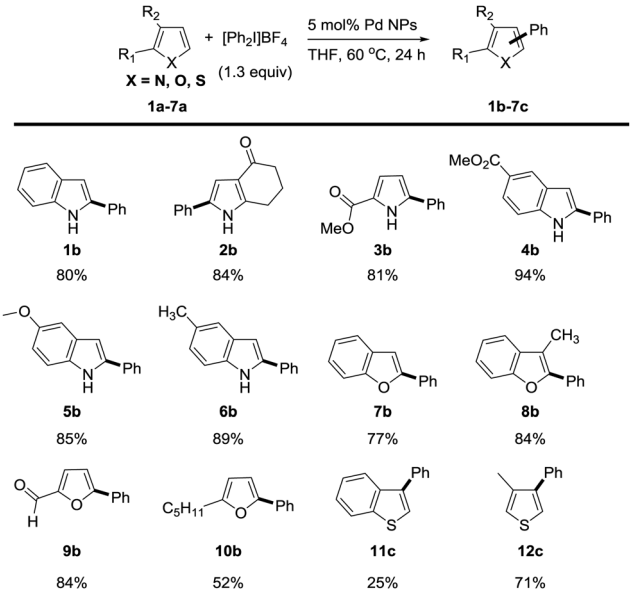

Scheme 1 Substrate scope of indoles, furans, and thiophenes. [a] Conditions: indole (0.2 mmol), $[Ph_2I]BF_4$ (0.26 mmol) and solvent (2.0 mL) without exclusion of air and moisture. Isolated yields are given.

(**1a**), 1,5,6,7-tetrahydro-4*H*-indol-4-one (**2a**), methyl 2-carboxylate pyrrole (**3a**), methyl 1*H*-indole-5-carboxylate (**4a**) 5-methoxy-1*H*-indole (**5a**) and 5-methyl-1*H*-indole (**6a**) transformed into the corresponding phenylated products in 80%, 84%, 81%, 94%, 85% and 89% yields, respectively. Remarkably, the C2 arylation products were exclusively generated over the C3 arylation ones in excellent regioselectivities of $>99:1$ in all reactions. O-Heterocyclic compounds such as benzofuran (**7a**), 3-methyl benzofuran (**8a**), 2-furaldehyde (**9a**), and 2-pentylfuran (**10a**) also provided the C2 arylation products (**7b–10b**) with excellent regioselectivity in 77%, 84%, 84%, and 52% yields, respectively. In the case of C–H arylation of sulfur-containing heterocycles, benzo[*b*]thiophene (**11a**) was not effective (25% yield), but 3-methylthiophene (**12a**) provided the C3-arylated product (**12c**) with good yield of 71%. Both sulfur-containing heterocycles showed the regioselectivity at the C3 position ($>99:1$) in accordance with the literature.[16]

To confirm the involvement of the heterogeneous catalytic species in the Pd NPs-catalyzed C–H arylation, we performed hot filtration and mercury poisoning tests.[27] The reaction mixture at 60 °C was filtered, and the filtrate did not contain any trace of Pd species over the detection limit (<0.01 ppm) analyzed by inductively coupled plasma-optical emission spectrometry (ICP-OES) (Fig. S5, ESI†). The addition of **2a** and $[Ph_2I]BF_4$ into the filtrate did not proceed the reaction at all at 60 °C for 6 h, also supporting the absence of the catalytic Pd species in the filtrate. For the mercury poisoning test, a drop of mercury to the reaction mixture of **2b** completely stopped the reaction (Fig. S6, ESI†). These control experiments indicate that the C–H arylation mainly occurred by the heterogeneous catalytic species of the Pd NPs.[15,16]

Generally, the heterogeneous catalyst has a high level of reusability compared to the homogeneous catalyst. After the reaction, the Pd NPs were recovered and reused five more times.

The recycle experiments provided the arylated product within the narrow range of 80–86% conversions under 6 cycles (Fig. S7, ESI†). After the recycling experiments, the morphology of the catalyst was preserved as the original spherical structure well. Because only the surface was oxidized to form active species, the original hardy Pd(0) frameworks of the catalysts may lead to a high degree of reliability (see below).

Under the present oxidative reaction conditions, Pd(0) species are easily oxidizable to Pd(II) or Pd(IV) species. To clarify the oxidation states of Pd NPs during the reaction, the Pd NPs were treated with $[Ph_2I]BF_4$ in THF at 60 °C without the substrates. The X-ray photoelectron spectroscopy (XPS) shows that the pristine Pd NPs have the major two peaks at 340.2 and 335.8 eV in the Pd 3d region, corresponding to Pd(0) species (Fig. 1c, green).[28] After the treatment, two new peaks distinctively emerge at 341.8 and 336.7 eV (Fig. 1d, blue), indicating the formation of Pd(II) species by surface oxidation.[29] The infrared spectroscopy of the oxidized NPs showed that a new peak appeared at 730 cm^{-1}, correlated with the typical out of plane bending peak of monosubstituted rings (Fig. S8, ESI†).[30] These measurements reveal the existence of Ph–Pd(II) species under the reaction conditions.

X-ray absorption spectroscopy provides direct information of the oxidation state and coordination environment at the metal centres.[31] In X-ray absorption near-edge structure (XANES), the characteristic white line at 24 370 eV with the subsequent pattern at 24 388 eV for oxidized Pd NPs (red) is close to that of the pristine Pd NPs (green), rather than the intense peak at 24 371 eV of PdO (black). It indicates that the major fraction of the oxidized Pd NPs still involves Pd(0) species (Fig. 2a). The Fourier transform of k^2-weighted Pd K-edge extended X-ray absorption fine structure (EXAFS), however, shows significantly distinct features from Pd(0) (Fig. 2b and Fig. S9, ESI†). The pristine Pd NPs show a strong single peak (green) identical to that of Pd foils, which corresponds to the Pd–Pd bond length at 2.7 Å. The coordination number of the Pd–Pd bond was simulated to be 5.0 due to the less-coordinated surface sites exposed outward (Fig. 2c). On the other hand, the oxidized Pd NPs (red) have distinct signals at 1.6–2.2 Å, corresponding to the overlaps of Pd–C and Pd–O bonds, prior to the strong peak for the Pd–Pd bond. Using the average Pd–C and Pd–O bond lengths observed in organometallic compounds,[32,33] the optimal fitting provided the coordination numbers of Pd–Pd, Pd–C, and Pd–O to be 4.8, 1.2, and 1.1, respectively (Fig. 2c). Based on these spectroscopic measurements, it is reasonable to identify that the oxidized NPs are composed of polymeric aryl–Pd(II)–oxo clusters, –(Pd(II)(Ph)–O)–, bearing both Pd–Ph and Pd–O bonds. The charge of Pd(II) was stabilized by the coordination of aryl and oxo ligands. The large fraction of the Pd species is still Pd(0), indicating that the pristine Pd NPs are partially oxidized by $[Ph_2I]BF_4$. The oxidized domains are potentially located at the surface, in consideration of the coordination number (4.8) of Pd–Pd bonds nearly identical to that of the pristine NPs and large Pd(II) peaks in the XPS spectrum. These aryl–Pd(II)–oxo clusters are robust in aprotic solvents such as THF and retain their nanoscale morphology.

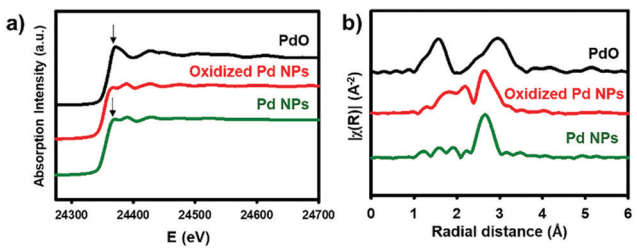

c)

	Bond	C.N.[a]	r (nm)[b]	σ^2 (pm^2)[c]	R-factor
Pd NPs	Pd-Pd	5.0±0.4	0.274±0.003	10±0.8	0.012
Oxidized Pd NPs	Pd-Pd	4.8±0.9	0.274±0.017	10±1	
	Pd-C	1.2±0.1	0.199±0.005	16±3	0.013
	Pd-O	1.1±0.1	0.212±0.006	51±24	

[a] Coordination number. [b] Bond distance. [c] Debye-Waller factors.

Fig. 2 (a) Pd K-edge XANES and (b) FT of k^2-weighted Pd K-edge EXAFS spectra. (c) Structural parameters obtained from the EXAFS refinement.

To propose the catalytic mechanism of C–H arylation, a model reaction, arylation of indole (**1a**), was selected. To demonstrate the arylation reactions that occurred on the surface of Pd(II) with phenyl, we performed three control experiments. First, the catalytic arylation was carried out with excess indole (5 equiv.) in the presence of $[Ph_2I]BF_4$ (1 equiv.). The arylated product (**1c**) was isolated in 15% yield. Then the surface oxidation states of Pd NPs were characterized by XPS. The spectrum at the Pd 3d level after the arylation showed the large decrease of Pd(II) (Fig. 3a and b). It evidenced that coordinated phenyl groups on the Pd(II) surface were used as arylation sources. Second, the mixture of Pd NPs and $[Ph_2I]BF_4$ were heated to 60 °C for 24 h in THF. After the reaction, biphenyl was solely yielded without the original substrates (Fig. S10, ESI†). In comparison, the biphenyl compounds were not detected without Pd NPs. These results confirmed the formation of Pd(II)–aryl species during the reaction.[34] Third, the addition of H_2O increased the product yields (Fig. S11, ESI†) and the fraction of Pd(II) species in the XPS spectrum (Fig. S12, ESI†). However, the addition of O_2 did not affect the yield. Thus, we could rationally propose that H_2O participates in the catalyst generation and the C–H arylation. As a result, we propose a plausible catalytic cycle for the C–H arylation on the heterogeneous Pd (Fig. 3c). The surface of Pd NPs is oxidized to generate –(Pd(II)(Ph)O)– clusters (**II**), which mediate C–H activation to form the intermediate (**III**). The subsequent reductive elimination provides the intermediate (**IV**), which is further oxidized to the –(Pd(II)(Ph)O)– clusters (**II**) by the action of $[Ph_2I]BF_4$ and H_2O.

In conclusion, we investigated the heterogeneous catalytic system promoting C–H arylation reactions of heterocycle compounds in high yield and regioselectivity. Multiple spectroscopic analyses revealed that the oxidized Pd(II) intermediates were –(Pd(II)(Ph)O)– clusters generated on the Pd(0) surface. Such heterogeneous Pd(II) species are expected to additional features superior to homogeneous catalysis, including easy access to regioselectively demanded substrates. These heterogeneous catalytic systems with

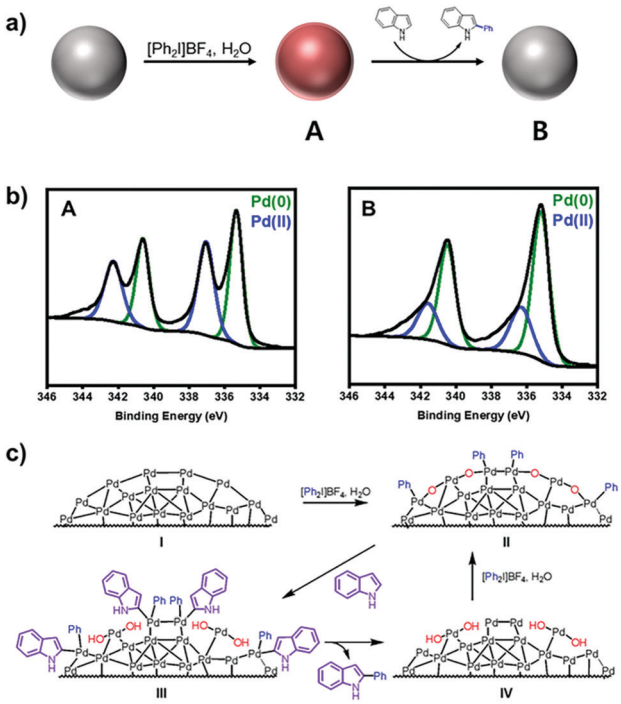

Fig. 3 (a) Reaction scheme and (b) XPS spectra at the Pd 3d level of (A) oxidized Pd NPs after the treatment with $[Ph_2I]BF_4$ and (B) after C–H arylation in air. (c) Proposed catalytic cycle.

homogeneous substrates would offer synergistic characteristics merging the advantages of both systems, such as enhanced catalytic performances with separation and recycle abilities.

This work was supported by Saudi Aramco-KAIST CO_2 management center. The authors thank for the support by the National Research Foundation of Korea (NRF) funded by the Korea Government (MSIT) (2018R1A2B3004096, 2018R1A5A1025208, and 2020 R1A2C2013420). SJC thanks the Global Frontier Center for Hybrid Interface Materials (GFHIM, grant no. NRF-2015M3A6B106526633). The authors acknowledge the Pohang Accelerator Laboratory (PAL) for beamline use. EXAFS experiments at PLS were supported by MSIP and POSTECH.

Conflicts of interest

The authors declare no conflict of interest.

Notes and references

1 A. Biffis, P. Centomo, A. D. Zotto and M. Zecca, *Chem. Rev.*, 2018, **118**, 2249–2295.
2 L. X. Yin and J. Liebscher, *Chem. Rev.*, 2007, **107**, 133–173.
3 Y. Zhao, L. Du, H. Li, W. Xie and J. Chen, *J. Phys. Chem. Lett.*, 2019, **10**, 1286–1291.
4 S. Shabbir, S. Lee, M. Lim, H. Lee, H. Ko, Y. Lee and H. Rhee, *J. Organomet. Chem.*, 2017, **846**, 296–304.
5 S. Santoro, S. I. Kozhushkov, L. Ackermann and L. Vaccaro, *Green Chem.*, 2016, **18**, 3471–3493.
6 A. J. Reay and L. J. S. Fairlamb, *Chem. Commun.*, 2015, **51**, 16289–16307.
7 L. Djakovitch and F.-X. Felpin, *ChemCatChem*, 2014, **6**, 2175–2187.
8 D. Pla and M. Gómez, *ACS Catal.*, 2016, **6**, 3537–3552.
9 L. J. S. Fairlamb, A. R. Kapdi, A. F. Lee, G. Sanchez, G. Lopez, J. L. Serrano, L. Garcia, J. Perez and E. Perez, *Dalton Trans.*, 2004, 3970–3981.
10 A. H. M. de Vries, J. M. C. A. Mulders, J. H. M. Mommers, H. J. W. Henderckx and J. G. de Vries, *Org. Lett.*, 2003, **5**, 3285–3288.
11 C. Deraedt and D. Astruc, *Acc. Chem. Res.*, 2014, **47**, 494–503.
12 M. T. Reetz and J. G. de Vries, *Chem. Commun.*, 2004, 1559–1563.
13 J. G. de Vries, *Dalton Trans.*, 2006, 421–429.
14 T. E. Storr, C. G. Baumann, R. J. Thatcher, S. D. Ornellas, A. C. Whitwood and L. J. S. Fairlamb, *J. Org. Chem.*, 2009, **74**, 5810–5821.
15 K. D. Collins, R. Honeker, S. Vásquez-Céspedes, D.-T. D. Tang and F. Glorius, *Chem. Sci.*, 2015, **6**, 1816–1824.
16 D.-T. D. Tang, K. D. Collins, J. B. Ernst and F. Glorius, *Angew. Chem., Int. Ed.*, 2014, **53**, 1809–1813.
17 D.-T. D. Tang, K. D. Collins and F. Glorius, *J. Am. Chem. Soc.*, 2013, **135**, 7450–7453.
18 R. Ye, A. V. Zhukhovitskiy, C. V. Deraedt, F. D. Toste and G. A. Somorjai, *Acc. Chem. Res.*, 2017, **50**, 1894–1901.
19 C. Deraedt, R. Ye, W. T. Ralston, F. D. Toste and G. A. Somorjai, *J. Am. Chem. Soc.*, 2017, **139**, 18084–18092.
20 A. J. Brown, D. Pinkowicz, M. R. Saber and K. R. Dunbar, *Angew. Chem., Int. Ed.*, 2015, **52**, 5864–5868.
21 Y. Li, J. H.-C. Liu, C. A. Witham, W. Huang, M. A. Marcus, S. C. Fakra, P. Alayoglu, Z. Zhu, C. M. Thompson, A. Arjun, K. Lee, E. Gross, F. D. Toste and G. A. Somorjai, *J. Am. Chem. Soc.*, 2011, **133**, 13527–13533.
22 K. Kim, Y. Jung, S. Lee, M. Kim, D. Shin, H. Byun, S. J. Cho, H. Song and H. Kim, *Angew. Chem., Int. Ed.*, 2017, **56**, 6952–6956.
23 M. Kim, S. Lee, K. Kim, D. Shin, H. Kim and H. Song, *Chem. Commun.*, 2014, **50**, 14938–14941.
24 M. Kim, J. C. Park, A. Kim, K. H. Park and H. Song, *Langmuir*, 2012, **28**, 6441–6447.
25 B. D. Hall, D. Zanchet and D. Ugarte, *J. Appl. Crystallogr.*, 2000, **33**, 1335–1341.
26 V. Arun, P. O. V. Reddy, M. Pilania and D. Kumar, *Eur. J. Org. Chem.*, 2016, 2096–2100.
27 R. H. Crabtree, *Chem. Rev.*, 2012, **112**, 1536–1554.
28 X. Fan, F. Wang, T. Zhu and H. He, *J. Environ. Sci.*, 2012, **24**(3), 507–511.
29 L. S. Kibis, A. I. Stadnichenko, S. V. Koscheev, V. I. Zaikovskii and A. I. Boronin, *J. Phys. Chem. C*, 2012, **116**, 19342–19348.
30 M. Margoshes and V. A. Fassel, *Spectrochim. Acta*, 1955, **7**, 14–24.
31 K. R. Priolkar, P. Bera, P. R. Sarode, M. S. Hegde, S. Emura, R. Kumashiro and N. P. Lalla, *Chem. Mater.*, 2002, **14**, 2120–2128.
32 P. L. Alsters, J. Boersma, W. J. J. Smeets, A. L. Spek and G. van Koten, *Organometallics*, 1993, **12**, 1639–1647.
33 J. M. Keith, W. A. Goddard and J. Oxgaard, *J. Am. Chem. Soc.*, 2007, **129**, 10361–10369.
34 Rearrangement of Pd(II)–Ph species could provide Ph–Pd(II)–Ph species, resulting in Pd(0) and biphenyl.